

RESEARCH ARTICLE

Relative abundance of *Bacillus* spp., surfactant-associated bacterium present in a natural sea slick observed by satellite SAR imagery over the Gulf of Mexico

Kathryn Lynn Howe*, Cayla Whitney Dean*, John Kluge*, Alexander Victor Soloviev*, Aurelien Tartar†, Mahmood Shivji†, Susanne Lehner‡ and William Perrie§

The damping of short gravity-capillary waves (Bragg waves) due to surfactant accumulation under low wind speed conditions results in the formation of natural sea slicks. These slicks are detectable visually and in synthetic aperture radar satellite imagery. Surfactants are produced by natural life processes of many marine organisms, including bacteria, phytoplankton, seaweed, and zooplankton. In this work, samples were collected in the Gulf of Mexico during a research cruise on the R/V *F.G. Walton Smith* to evaluate the relative abundance of *Bacillus* spp., surfactant-associated bacteria, in the sea surface microlayer compared to the subsurface water at 0.2 m depth. A method to reduce potential contamination of microlayer samples during their collection on polycarbonate filters was implemented and advanced, including increasing the number of successive samples per location and changing sample storage procedures. By using DNA analysis (real-time polymerase chain reaction) to target *Bacillus* spp., we found that in the slick areas, these surfactant-associated bacteria tended to reside mostly in subsurface waters, lending support to the concept that the surfactants they may produce move to the surface where they accumulate under calm conditions and enrich the sea surface microlayer.

Keywords: microlayer; surfactant; bacteria; SAR

Introduction

Under low wind speed conditions, organic material, including surface-active compounds (surfactants), accumulate and form sea slicks. Surfactants cause dampening of short, gravity-capillary waves (Bragg waves), enabling the resulting sea slicks to be detected both visually and in optical and synthetic aperture radar (SAR) satellite imagery. There are many causes for the accumulation of natural surfactants on the sea surface: build-up of organic material; terrestrial runoff (Wurl et al., 2011); oceanic features, such as convergence zones or frontal interfaces (Gade et al., 2013); high biological productivity; and sediment upwelling/resuspension (Espedal et al., 1996). Natural slicks and microbial communities are believed

to be highly variable in time and space, and can be easily disturbed by increased wind speeds or wave breaking. Sea slicks are of interest because they influence gas exchange rates at the air-sea interface (Cunliffe et al., 2011).

Many marine organisms, including phytoplankton, zooplankton, seaweed, and bacteria, produce surfactants during various life processes (Gade et al., 2013). Bacteria produce surfactants for nutrient acquisition, hydrocarbon degradation, cell-to-cell communication, biofilm formation/inhibition, toxin isolation, and antifungal and antiviral activities (Dinamarca et al., 2013). Surfactants are amphiphilic compounds composed of various phospholipids, glycolipids, lipopeptides, fatty acids, and other complex molecules. The amount and type of surfactant produced depends on many factors, including availability of nutrients, such as nitrogen, magnesium, and potassium, as well as the environmental factors of pH, temperature, and salinity (Karanth et al., 1999).

The marine bacterial genera that are well-known for producing, degrading, or having some other association with surfactants include *Pseudomonas*, *Bacillus*, *Corynebacterium*, and *Acinetobacter* (Satpute et al., 2010; Sekhon et al., 2012). Knowing the abundance and diversity of these bacteria, especially in boundary layers such as

* Nova Southeastern University, Department of Marine and Environmental Sciences, Dania Beach, FL, US

† Nova Southeastern University, Department of Biological Sciences, Ft. Lauderdale, FL, US

‡ German Aerospace Center (DLR) Remote Sensing Technology Institute, Oberpfaffenhofen, DE

§ Bedford Institute of Oceanography, Bedford, NS, CA

Corresponding author: Kathryn Lynn Howe (klh17f@my.fsu.edu)

the air-sea interface, can help to build a knowledge base towards understanding surfactant accumulation in the sea surface microlayer (SML). The previous work of Kurata et al. (2016) found that in the slick areas they examined, surfactant-associated bacteria resided mostly in subsurface waters, potentially producing surfactants that could move to the surface and enrich the SML. Such enrichment is consistent with the experimental results of Cunliffe et al. (2011) and Wurl et al. (2011), which showed enrichment of organic matter and surfactants in the SML.

In this study, satellite SAR imagery was used to visualize slicks on the sea surface and relate them to the potential presence of surfactant-associated bacteria. The activity of surfactant-associated bacteria is not detected by satellite sensors (ocean color or SAR images), but the accumulation of surfactants can be inferred from SAR images that show the presence of surface slicks (Kurata et al., 2016; Hamilton et al., 2015a; Soloviev and Lukas, 2014). SAR satellites can image the sea surface in both daytime and nighttime conditions, because the SAR technology is based on microwaves that can penetrate cloud cover and fog. Recently, high resolution SAR satellites, like TerraSAR-X and RADARSAT-2, have been used to image highly variable coastal and oceanographic processes; these images are available to the scientific community (see, e.g., <http://terrasar-x.dlr.de>). As the SAR satellite images the sea surface, a normalized calibrated radar backscatter can be used to measure the roughness of the sea surface, which correlates to wind speed (Lehner et al., 1998). The roughness of the surface is not just dependent on the wind speed; surfactants or oil spills can dampen the short gravity-capillary waves, as well. This dampening causes slicks to appear as darker areas in SAR imagery as the slick reflects the microwaves away from the receiving antenna, compared to the surrounding rougher sea surface. In addition to biogenic slicks, other features such as oil spills, grease ice, wind shadowing/sheltering (Soloviev et al., 2010), rain, ship wakes, and internal waves (Velotto et al., 2011) can cause dark patches in SAR imagery. Man-made ocean metallic targets (oil rigs, ships, etc.) are easily observed in SAR imagery as bright pixels because of their strong backscatter coefficient. Another feature on SAR satellite imagery is speckle, which is the effect of coherent summation and subtraction of the radar signal (amplitude and phase) inside the resolution cell. Speckle gives the noisy “salt-and-pepper” aspect to SAR images which can be reduced by averaging more statistically independent pixels.

The targeted environment of this study was the sea surface microlayer (SML) and associated subsurface water (SSW). The SML covers approximately 70% of the Earth's surface and is the boundary between the atmosphere and ocean where many biogeochemical processes occur (Liss and Duce, 1997). It is considered an extreme environment due to high variability in fluxes of nutrients, salinity, temperature, radiation (solar and UV), heat, momentum, and gas (Maki, 1993; Liss and Duce, 1997). The biogeochemical processes occurring at the air-sea interface are influenced by exchanges between the SML and both the subsurface water and atmosphere. Particles from the atmosphere, for

instance aerosols and dust, are deposited into the SML from the air side of the air-sea interface. Marine organisms at this boundary can either be persistent residents of the SML (bacteria, phytoplankton, zooplankton) or temporary inhabitants (fish eggs, invertebrate larvae).

There have been several attempts to define the exact structure of the SML. Hardy (1982) depicted the SML as having distinct, stratified layers in which surfactants, lipids, and alcohols are fixed above a protein and carbohydrate layer. Current models show a lesser degree of organic organization, with gel-like particles and bacteria mixed heterogeneously in the upper portion of the microlayer (Cunliffe et al., 2011). The physical structure of the SML includes aqueous molecular sublayers, each starting at the air-sea interface: the viscous sublayer (~1500 μm thick), thermal sublayer (~500 μm thick), and salinity and gas diffusion sublayer (~50 μm thick). These sublayers are characterized by significant gradients in current velocity, temperature, and gas concentration, which pose challenges to organisms that reside in the ocean surface (Soloviev and Lukas, 2014).

Several techniques have been developed to sample the microlayer, including the use of membrane filters (hydrophilic and hydrophobic), glass plates, mesh screens (metal or nylon), and rotating drums. Each technique involves a sampling depth of different thickness. For example, membrane filters can sample thicknesses of 6 to 42 μm , while glass plates sample from 20 to 150 μm and mesh screens from 150 to 400 μm (Cunliffe and Wurl, 2014; Cunliffe et al., 2009). The sampling depth of the hydrophilic polycarbonate (47-mm diameter) filter used in this study has been estimated by obtaining a mean value for the amount of water removed from the sea surface on the filter and calculating the thickness/depth of the sample using the surface area of the filter, which yielded an average sampling depth of $35 \pm 5 \mu\text{m}$ ($n = 5$; Franklin et al., 2005). Depths of subsurface water samples included in studies of the SML can also vary from 0.1 to 20 m, depending on whether bottles, pumps or rosettes are used as the sampling device (Cunliffe and Wurl, 2014). The discrepancies in sampling depths among the different methods makes comparing microlayer community composition between studies very difficult. Franklin et al. (2005) proposed using membrane filters for bacterial studies, as they are less susceptible to contamination especially in experiments involving the polymerase chain reaction (PCR).

In this work, we have implemented the membrane-filter method of Franklin et al. (2005) for sea surface microlayer sampling. Franklin et al. (2005), however, did their sampling from a boat in calm conditions. Hamilton et al. (2015a, 2015b) and Kurata et al. (2016) advanced the use of this technique by extending the range of sea state conditions. This paper, while similar to the previous work of Hamilton et al. (2015a, 2015b) and Kurata et al. (2016), differs by sampling a new location (in the Gulf of Mexico) and thus expanding the geographic relevance of results from these types of analyses. The number of samples collected was also increased to improve statistical power, and the quantitative PCR (qPCR) method used to evaluate

abundance of the targeted organisms was modified by using the Pfaffl (2001) method (see Eq. 1).

Methods

Over 100 samples were collected in the Gulf of Mexico in February 2016 during a Gulf of Mexico Research Initiative (GoMRI) research cruise for the LAGRANGIAN Submesoscale Experiment (LASER) of the Consortium for Advanced Research on the Transport of Hydrocarbons in the Environment (CARTHE) (Table 1). The sampling on February 10 was by small boat at a nearshore location in brown water of the Mississippi River plume, while sampling on February 6 and 12 was conducted from the R/V *F.G. Walton Smith* in close proximity to the Deepwater Horizon site (Figure 1). All sampling was recorded on video using a GoPro camera to identify sea state, possible instances of contamination, and folding/submersion of the filter during sampling. All questionable samples (possibly contaminated or on compromised filters) were removed from analysis. Wind speed was recorded by the anemometer on board the R/V *F.G. Walton Smith*.

The membrane-filter method of Franklin et al. (2005) for sampling the SML, as expanded upon by Kurata et al. (2016), was implemented in this study in order to decrease contamination of the sample by the ship wake, boat, and researcher. A hydrophilic polycarbonate membrane filter was attached to a sterile hook and line, which was then stored in a sterile bag until ready for deployment in the field. A fly-fishing technique using a ten-foot fishing pole was used to reach an area outside the ship's wake to lay the filter on the ocean surface for three to five seconds. Using the fishing pole, the filter was lifted off the surface and caught using sterile forceps. This study enhanced contamination safeguards and sample collection/storage methods in comparison to Kurata et al. (2016); for example, the filter was placed directly in a labeled MoBio bead tube, which was later used for DNA extraction. This approach ensured that there was no loss of sample material, which is vital as only a small amount of material is collected on the filters. While the filter limits the amount of sample that is collected, it is a reliable, fine-scale method to study microbes in the sea surface microlayer. Samples were held on ice in the field and transferred to a -80°C

freezer where they were stored until extraction. Storage time in the -80°C ranged from several hours to five days.

The SSW was sampled at 0.2 m, using a peristaltic pump with tubing sterilized with 90% isopropanol and then rinsed with SSW. After approximately 45s of SSW flowing through the tube, the water sample was collected in a sterile bag. A filter, which had been stored in a sterile bag, was dipped in the water sample using sterile forceps, swirled around, and then placed in a labeled MoBio bead tube for subsequent DNA extraction. Samples were held on ice in the field and then placed in a -80°C freezer until extraction.

Control filters were collected as a baseline for DNA analysis by qPCR and analyzed for possible contamination. Air-control filters were exposed to the air at the sampling site for approximately 30 s. Non-exposed control filters consisted of filters originally prepared for SSW samples that were only taken out of the sterile bag immediately prior to extraction. Non-template controls, using only PCR water and no filter, were also analyzed.

The sampling conducted on February 12 occurred several hours after a TerraSAR-X satellite overpass. The TerraSAR-X stripmap intensity image shows a well-defined convergence zone in the sampling area on February 12, represented by the linear dark elongated area and surrounding dark areas in the middle of the SAR image (Figure 2). Convergence zones associated with downwelling are known for the accumulation of organic matter and microbial life and thus the formation of slicks (Espedal and Johannessen, 1996). Some oil seeps might have also contributed to this slick, but the presence of oil was not detectable visually in the SML sampling area. A small dark scar on the southern side of the convergence zone, however, indicated a possible oil spill of unknown origin. The rougher water in the SAR image indicated the presence of atmospheric convective cells due to warmer temperature on the southern side of the front.

DNA extraction was performed using a MoBio PowerWater DNA Isolation Kit, following the associated protocol (MoBio Laboratories, Inc., Carlsbad, CA). Quantitative polymerase chain reaction (qPCR), the real-time monitoring of the amplification of a target gene, was performed on the extracted, non-purified DNA on a LightCycler 96 (Roche Diagnostics International Ltd.,

Table 1: Sample collection information. DOI: <https://doi.org/10.1525/elementa.268.t1>

Site	Date (2016)	Slick present	Wind speed (m s^{-1})	Sampling platform	Number of samples	
					SML	SSW
1	Feb 6	No	4–5	Small boat	7	0
2	Feb 6	No	7–8	Small boat	8	6
3	Feb 6	No	5–7	Small boat	11	9
4	Feb 10	No	5–7	R/V <i>F.G. Walton Smith</i>	9	3
5	Feb 10	No	7–8	R/V <i>F.G. Walton Smith</i>	9	3
6	Feb 12	Yes	2–3	R/V <i>F.G. Walton Smith</i>	11	9
7	Feb 12	Yes	2–3	R/V <i>F.G. Walton Smith</i>	10	9



Figure 1: Sampling sites and dates in the Gulf of Mexico. Samples were collected during the 2016 GoMRI LASER research cruise. DWH refers to the Deepwater Horizon site. DOI: <https://doi.org/10.1525/elementa.268.f1>

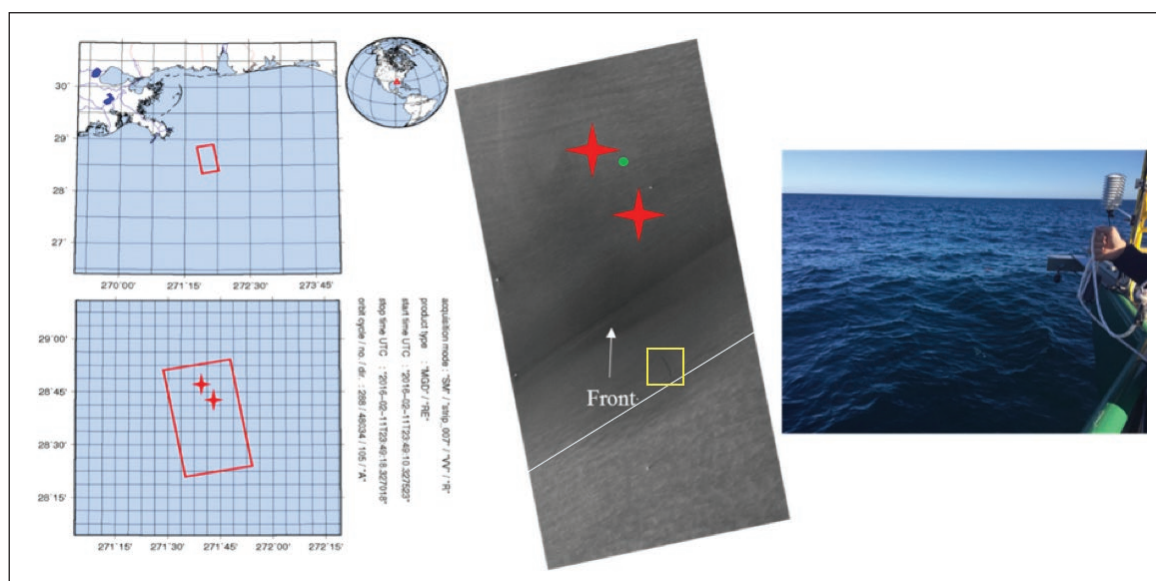


Figure 2: Reference map, satellite image and photograph of a sea surface slick on February 11, 2016. Reference map (left) for TerraSAR-X stripmap intensity image (middle) acquired on February 11, 2016, at 23:49:10 UTC, with sampling sites 6 and 7 on February 12 (Table 1) denoted by red stars. The dark elongated area and surrounding dark areas in the middle of the SAR image show the slick accumulating at the convergence zone, while the lighter area in the south indicates rougher water. Bright spots in the image are oil rigs. In the photograph (right), the lighter area shows the slick on February 12, 2016, at 15:05:43 UTC in the SML sampling area. The area above the white line indicates the slick areas in the SAR image. The yellow rectangle contains the area of the possible oil spill. The green dot indicates where the photograph on the right was taken. DOI: <https://doi.org/10.1525/elementa.268.f2>

Indianapolis, IN). Real-time monitoring refers to the fact that a fluorescent dye is included in the PCR mix so that when it binds to double-stranded DNA, it fluoresces, and the LightCycler plots fluorescence versus cycle number after each cycle. The more fluorescence, the more target gene is present. **Figure 3** shows an example of a qPCR plot from this study, with fluorescence on the y-axis and cycle number on the x-axis. A FastStart Essential DNA Green Master (Roche Diagnostics International Ltd., Indianapolis, IN), specifically designed for the LightCycler 96, contained the reagents for the master mix, including SYBR Green I, which is the fluorescent dye. This fluorescence is sequence-independent, meaning that primer-dimers, inadequate primer concentration, and secondary metabolites could cause the dye to bind to double-stranded DNA and fluoresce (Ponchel et al., 2003). The master mix,

modified from Hamilton et al. (2015a and 2015b), contained 12.5 μL SYBR-Green 1, 8.5 μL PCR water, 1 μL of 10 μM Bac265F, and 1 μL of 10 μM Bac525R. Bac265F and Bac525R are primers designed to amplify 16 s rRNA gene sequences specific to the genus *Bacillus* (Xiao et al., 2011). qPCR runs for sampling Sites 2–5 contained 2.5 μL of DNA, while Sites 6 and 7 contained only 2 μL of DNA. All samples were run in duplicate.

The qPCR protocol, which has been modified from Hamilton et al. (2015a and 2015b), had an initial denaturing step of 95°C for 15 min, followed by 25 cycles of 94°C for 30 s, 62°C for 30 s, and 72°C for 2 min, followed by an extension at 72°C for 10 min followed by a melt curve. Each sampling day was analyzed in a separate qPCR run (Table S1). We applied the Pfaffl method (Pfaffl, 2001), which uses the ratio of quantified target gene to reference

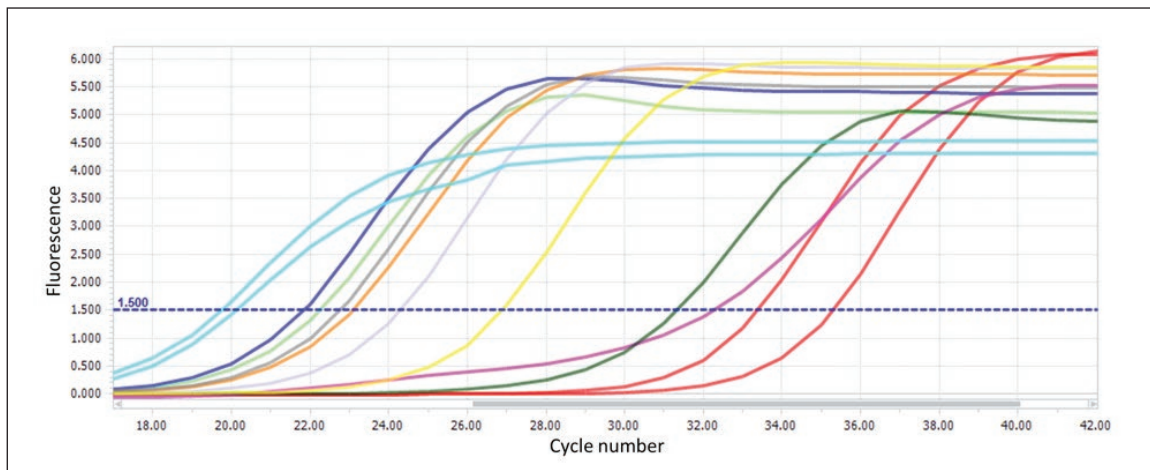


Figure 3: An example of a qPCR amplification plot from Site 3. This plot of fluorescence versus cycle number shows curves for the positive controls (bright blue, far left, cultured *Bacillus cereus*), negative controls (red, far right, NTC), and (left to right.) SSW samples (dark blue, light green), SML samples (gray, orange, light purple, yellow, dark green), and an air control (bright pink) from Site 3. The cycle number values corresponding with the threshold at 1.5 for the linear phase of amplification (blue dashed line) were used for abundance calculations. Primers specific to *Bacillus* spp. were used for all samples. DOI: <https://doi.org/10.1525/elementa.268.f3>

gene (rather than attempting to determine absolute number of the target gene), to obtain the expression ratio or “relative abundance” of *Bacillus* spp. in a given sample, according to this equation:

$$ratio = \frac{E_x^{\Delta CT_{target} (control - sample)}}{E_{NTC}^{\Delta CT_{ref} (control - sample)}} \quad (1)$$

In this method, the cycle number threshold (*CT*) is set based on the linear phase of amplification for each sample (*x*); in this case, 1.5 for all runs (**Figure 3**). In the equation, *E* is the real-time PCR efficiency of the target or reference (*ref*) gene, calculated according to Pfaffl (2001). Use of primers for the V3 and V4 regions of the 16S rRNA *Bacillus cereus* gene served as the target gene. The mean relative abundance of *Bacillus* spp. for SML and SSW at a given site was calculated from the expression ratios obtained for all samples of that water type at a given location. Outliers, which showed higher abundance than the positive controls or lower abundance than the negative or non-template controls (NTC), were removed. Confidence intervals were calculated at 70% using Student’s t-distribution coefficient due to the small sample sizes (**Table 1**).

Results

The qPCR results depicted in **Figure 4** elucidate the differences in the mean relative abundance of *Bacillus* spp. between the SML and SSW. Sites 3, 4, 5, and 6 showed a statistically significant difference in the relative abundance between the SML and SSW using the 70% confidence intervals. There was no statistically significant difference between SML and SSW at Site 2, which was sampled under the highest (still moderate) wind speed conditions encountered (7–8 m s⁻¹) with no visible slick, or at Site 7, which was sampled under the lowest wind speed conditions (2–3 m s⁻¹) with a visible slick. The conservative two-tailed Student’s t-test suggested that the difference

in the relative abundance between the SML and SSW was only statistically significant for Sites 4 (*p* < 0.05) and 6 (*p* < 0.001). For the further analysis, we have used the 70% confidence intervals.

Sites 3 and 4, which had moderate wind speeds of 5–7 m s⁻¹ and no visible slicks, showed higher relative abundance of *Bacillus* spp. in the SML compared to SSW. Site 5, with higher (still moderate) wind speeds of 7–8 m s⁻¹ and no visible slicks, showed more *Bacillus* spp. in the SSW compared to SML. Both Sites 4 and 5 were sampled in brown water of the Mississippi River plume. Site 6, with lower wind speeds of 2–3 m s⁻¹, had a visible slick; there, the relative abundance of *Bacillus* spp. was higher in the SSW compared to the SML. Note that Site 1 was not considered in this analysis because only SML samples were taken at that location (no SSW data were available for comparison). There was significant variability in the relative abundance of *Bacillus* spp. for both the SML and SSW samples, similar to that observed in the previous work of Hamilton et al. (2015a).

Discussion

Our experimental results from qPCR analysis can be summarized as follows. Four sites showed statistically significant differences in relative abundance of *Bacillus* spp. in the SML compared to SSW: Site 6, sampled under low wind-speed conditions; and Sites 3, 4, and 5, sampled under moderate wind-speed conditions. Two sites did not produce statistically significant differences between the SML and SSW: Sites 2 and 7, sampled under moderate and low wind-speed conditions, respectively. Sampling in the brown water of the Mississippi River outflow under moderate wind conditions yielded variable results: Site 4 showed higher relative abundance of *Bacillus* spp. in the SML, while Site 5 showed higher abundance in the SSW. At the two sites characterized by calm conditions and the presence of slicks, the relative abundance of *Bacillus*

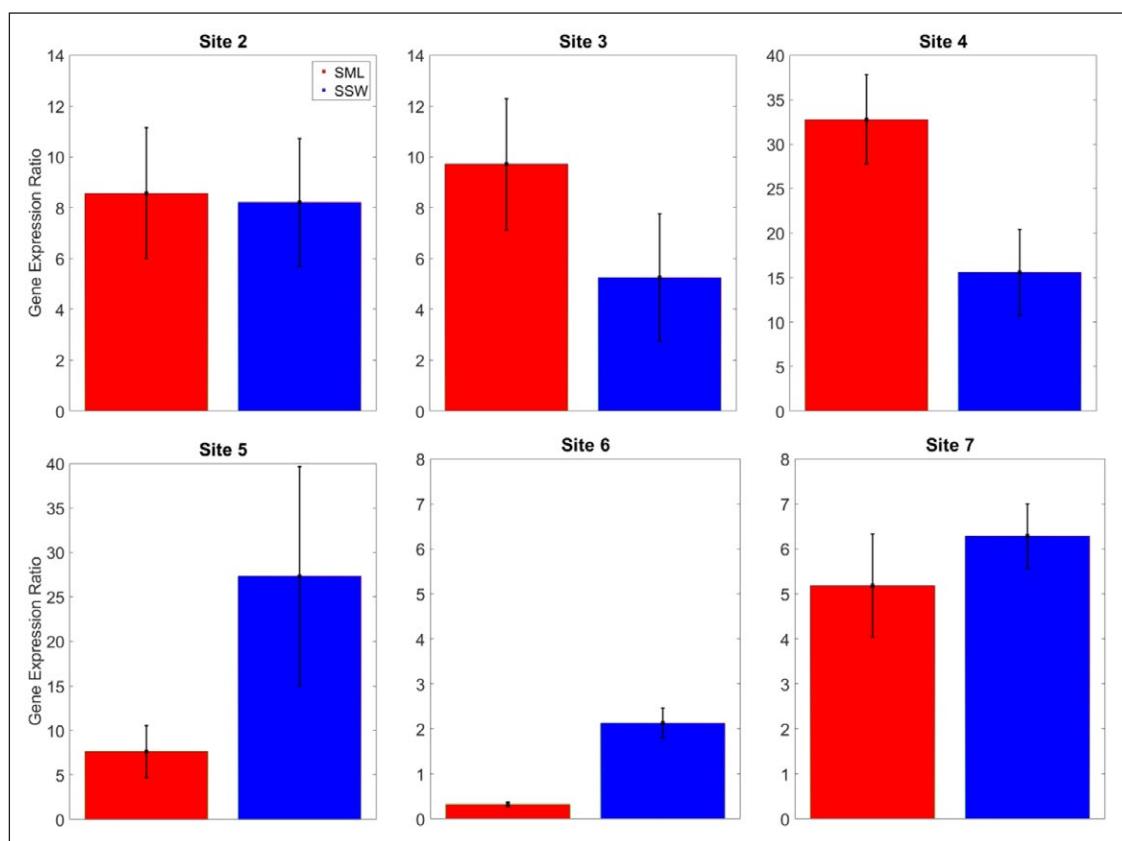


Figure 4: Mean relative abundance of *Bacillus* spp. in the SML and SSW samples collected in this study. Mean ratios of quantified target to reference genes (Equation 1) are given for each sample type (red bars for sea surface microlayer, SML; blue bars for subsurface water, SSW) as an indication of relative abundance of *Bacillus* spp. Note the differences in scale between panels. Error bars indicate 70% confidence intervals (n values given in Table 1). Samples were collected in the Gulf of Mexico during the 2016 LASER research cruise. DOI: <https://doi.org/10.1525/elementa.268.f4>

spp. was either significantly higher in SSW (Site 6) or else tended to be higher (Site 7). (Note that the relative abundance of *Bacillus* spp. was, in general, smaller under moderate rather than low wind speed conditions.) Although the number of successive SML samples was increased from the four to six in Kurata et al. (2016) and Hamilton et al. (2015a) to as many as ten in this study, statistical power for comparative purposes could have been improved further by increasing the number of SSW samples to ten as well. Increasing the number of successive samples above ten, however, would not have been feasible using the improved membrane-filter method of this study, as the ship drifted and would have left the site or slick area before such an extended sampling set could be completed.

Our results underscore the variability inherent to the SML-SSW system, while also suggesting that under calm weather conditions, more *Bacillus* spp., well-known surfactant-associated bacteria, tend to be present in the SSW compared to the SML. This conclusion is consistent with observations by Hamilton et al. (2015a and 2015b) and Kurata et al. (2016). It is also consistent with the understanding that surfactants may be produced in SSW and transported to the SML via physical processes such as advection, bubble scavenging, and convection, accumulating on and enriching the sea surface microlayer (Cunliffe et al., 2011).

SAR technology can help to visualize the slick areas targeted by studies of surfactant-associated bacteria, as slicks may not be visible in ocean color satellite imagery. (Research on pigment formation in bacteria (Pane et al., 1996) may be needed to advance the study of bacteria at the sea surface using remote imagery). This SAR technology can thus help to track organic material, such as dissolved oil and other pollution, in the water column by the presence of surface slicks (Kurata et al., 2016). SAR can also identify natural slicks and guide studies of their microbial contents.

Conclusions

In this paper, we have advanced the sampling methodology of the sea surface microlayer by building on previous studies. In particular, we were able to increase the number of samples collected at each site, providing more statistical power than achieved previously. In addition, by placing the filters directly in bead tubes used for DNA extraction, we reduced sample loss. A new dataset using this advanced methodology was collected from the sea surface in regions of the Gulf of Mexico not previously sampled. From this dataset came new evidence that in slick areas, surfactant-associated bacteria (*Bacillus* spp.) may reside in the subsurface water, producing surfactants that move to the surface, accumulate on, and enrich the sea

surface microlayer. Although consistent with the findings of Cunliffe et al. (2011), our results were obtained with a completely different methodology. Because microbial communities in the ocean are highly variable in time and space, replicating similar studies in new areas is needed to advance tests of hypotheses about transport and aggregation of surfactant-associated bacteria, under both low and moderate wind speed conditions.

Data Accessibility Statement

Data are publicly available through the Gulf of Mexico Research Initiative Information & Data Cooperative (GRIIDC) at <https://data.gulfresearchinitiative.org> (doi:0.7266/N7GF0RJH, 10.7266/N7PV6HVX).

Acknowledgements

The work has been conducted under the auspices of the SCOR 141 working group “Sea Surface Microlayer” and the Gulf of Mexico Research Initiative (GoMRI).

Funding information

This project was funded by the Consortium for Advanced Research on Transport of Hydrocarbon in the Environment (CARTHE)/GoMRI. This research was also made possible by a grant from The Gulf of Mexico Research Initiative.

Competing interests

The authors have no competing interests to declare.

Author contributions

- Contributed to conception and design: AVS, KLH, CWD
- Contributed to acquisition of data: KLH, AVS, JK, SL, WP
- Contributed to analysis and interpretation of data: KLH, CWD, AVS, AT, MS, SL
- Drafted and/or revised the article: KLH, CWD, AVS, SL
- Approved the submitted version for publication: KLH, CWD, AVS, SL, JK, AT, MS, WP

References

- Cunliffe, M, Harrison, E, Salter, M, Schafer, H, Upstill-Goddard, RC and Murrell, JC** 2009 Comparison and validation of sampling strategies for the molecular microbial analysis of surface microlayers. *Aquat Microb Ecol* **57**: 69–77. DOI: <https://doi.org/10.3354/ame01330>
- Cunliffe, M, Upstill-Goddard, RC and Murrell, JC** 2011 Microbiology of aquatic surface microlayers. *FEMS Microbiol Rev* **35**: 233–246. DOI: <https://doi.org/10.1111/j.1574-6976.2010.00246.x>
- Cunliffe, M and Wurl, O** 2014 Guide to Best Practices to Study the Ocean’s Surface. SCOR. Occasional Publications of the Marine Biological Association of the United Kingdom, Plymouth, UK, 118.
- Dinamarca, MA, Ibacache-Quiroga, CJ, Ojeda, JR and Troncoso, JM** 2013 Marine microbial biosurfactants: biological functions and physical properties as the basis for innovations to prevent and treat infectious diseases in aquaculture. Méndez-Vilas, A (ed.), *Microbial Pathogens and Strategies for Combating Them: Science, Technology and Education*. FORMATEX.
- Espedal, HA and Johannessen, OM** 1996 Satellite detection of natural film on the ocean surface. *Geophys Res Lett* **23**: 3151–3154. DOI: <https://doi.org/10.1029/96GL03009>
- Franklin, MP, McDonald, IR, Bourne, DG, Owens, NJP, Upstill-Goddard, RC and Murrell, JC** 2005 Bacterial diversity in the bacterioneuston (sea surface microlayer): the bacterioneuston through the looking glass. *Environ Microbiol* **7**: 723–736. DOI: <https://doi.org/10.1111/j.1462-2920.2004.00736.x>
- Gade, M, Byfield, V, Ermakov, S, Lavrova, O and Mitnik, L** 2013 Slicks as indicators for marine processes. *Oceanography* **26**(2): 138–149. DOI: <https://doi.org/10.5670/oceanog.2013.39>
- Hamilton, B** 2015b DNA Analysis of Surfactant Associated Bacteria in the Sea Surface Microlayer in Application to Satellite Remote Sensing Techniques: Case Studies in the Straits of Florida and the Gulf of Mexico. Dania Beach, FL: Nova Southeastern University. Available at: http://nsuworks.nova.edu/cgi/view-content.cgi?article=1376&context=occ_stuetd.
- Hamilton, B, Dean, C, Kurata, N, Vella, K, Soloviev, A, et al.** 2015a Surfactant associated bacteria in the sea surface microlayer: Case studies in the Straits of Florida and the Gulf of Mexico. *Can J Remote Sens* **41**(2): 135–143. DOI: <https://doi.org/10.1080/07038992.2015.1048849>
- Hardy, JT** 1982 The sea-surface microlayer: biology, chemistry and anthropogenic enrichment. *Prog Oceanogr* **11**: 307–328. DOI: [https://doi.org/10.1016/0079-6611\(82\)90001-5](https://doi.org/10.1016/0079-6611(82)90001-5)
- Karanth, NGK, Deo, PG and Veena Nadig, NK** 1999 Microbial production of biosurfactants and their importance. *Curr Sci* **77**(1): 116–126, 166.
- Kurata, N, Vella, K, Hamilton, B, Shivji, M, Soloviev, A, et al.** 2016 Surfactant-associated bacteria in the near-surface layer of the ocean. *Nature* **6**: 19123. DOI: <https://doi.org/10.1038/srep19123>
- Lehner, S, Horstmann, J, Koch, W and Rosenthal, W** 1998 Mesoscale wind measurements using recalibrated ERS SAR images. *J Geophys Res* **103**(C4): 7847–7856. DOI: <https://doi.org/10.1029/97JC02726>
- Liss, PS and Duce, RA** 1997 The sea surface and global change. Cambridge University Press, Cambridge. DOI: <https://doi.org/10.1017/CBO9780511525025.006>
- Maki, J** 1993 The air-water interface as an extreme environment. In: Ford, TE (ed.), *Aquatic Microbiology: An Ecological Approach*, 409–439. Blackwell Sci. Publ. Oxford.
- Mo Bio Laboratories, Inc.** PowerWater DNA Isolation Kit Sample: Instruction Manual. Available at: <https://mobio.com/media/wysiwyg/pdfs/protocols/14900-S.pdf> Accessed January 11, 2016.

- Pane, L, Radin, L, Franconi, G and Carli, A** 1996 The carotenoid pigments of a marine *Bacillus firmus* strain. *Boll Soc Ital Biol Sper* **72**: 303–308.
- Pffafli, MW** 2001 A new mathematical model for relative quantification in real-time RT–PCR. *Nucleic Acids Res* **29**(9): e45. DOI: <https://doi.org/10.1093/nar/29.9.e45>
- Ponchel, F, Toomes, C, Bransfield, K, Leong, FT, Douglas, SH, et al.** 2003 Real-time PCR based on SYBR_Freen I fluorescence: An alternative to the TaqMan assay for a relative quantification of gene rearrangements, gene amplifications, and micro gene deletions. *BMC Biotechnol* **3**: 18 DOI: <https://doi.org/10.1186/1472-6750-3-18>
- Satpute, SK, Banat, IM, Dhakephalkar, PK, Banpurkar, AG and Chopade, BA** 2010 Biosurfactants, bioemulsifiers and exopolysaccharides from marine microorganisms. *Biotechnol Adv* **28**: 436–450. DOI: <https://doi.org/10.1016/j.biotechadv.2010.02.006>
- Sekhon, KK, Khanna, S and Cameotra, SS** 2012 Biosurfactant production and potential correlation with esterase activity. *Pet Environ Biotechnol* **3**(7). DOI: <https://doi.org/10.4172/2157-7463.1000133>
- Soloviev, AV, Gilman, M, Young, K, Bruschi, S and Lehner, S** 2010 Sonar measurements in ship wakes simultaneous with TerraSAR-X overpasses. *IEEE Trans Geosci Remote Sens* **48**: 841–851. DOI: <https://doi.org/10.1109/TGRS.2009.2032053>
- Soloviev, AV and Lukas, R** 2014 The Near-Surface Layer of the Ocean: Structure, Dynamics and Application. *Springer*, 537. DOI: <https://doi.org/10.1038/srep05306>
- Velotto, D, Migliaccio, M, Nunziata, F and Lehner, S** 2011 Dual polarized TerraSAR-X data for oil-spill observation. *IEEE Trans Geosci Remote Sens* **49**: 4751–4762. DOI: <https://doi.org/10.1109/TGRS.2011.2162960>
- Wurl, O, Wurl, E, Miller, L, Johnson, K and Vagle, S** 2011 Formation and global distribution of sea-surface microlayers. *Biogeosciences* **8**: 121–135. DOI: <https://doi.org/10.5194/bg-8-121-2011>
- Xiao, Y, Zeng, GM, Yang, ZH, Ma, YH, Huang, C, Shi, WJ, Xu, ZY, Huan, J and Fan, CZ** 2011 Effects of continuous thermophilic composting (ctc) on bacterial community in the active composting process. *Microbial Ecol* **62**(3): 599–608. DOI: <https://doi.org/10.1007/s00248-011-9882-z>

How to cite this article: Howe, KL, Dean, CW, Kluge, J, Soloviev, AV, Tartar, A, Shivji, M, Lehner, S and Perrie, W 2018 Relative abundance of *Bacillus* spp., surfactant-associated bacterium present in a natural sea slick observed by satellite SAR imagery over the Gulf of Mexico. *Elem Sci Anth*, 6: 8. DOI: <https://doi.org/10.1525/elementa.268>

Domain Editor-in-Chief: Jody W. Deming, University of Washington, US

Knowledge Domain: Ocean Science

Part of an *Elementa* Special Feature: The Sea Surface Microlayer – Linking the Ocean and Atmosphere

Submitted: 28 February 2017 **Accepted:** 28 November 2017 **Published:** 25 January 2018

Copyright: © 2018 The Author(s). This is an open-access article distributed under the terms of the Creative Commons Attribution 4.0 International License (CC-BY 4.0), which permits unrestricted use, distribution, and reproduction in any medium, provided the original author and source are credited. See <http://creativecommons.org/licenses/by/4.0/>.

